Eur. Phys. J. D **44**, 547–556 (2007)
DOI: 10.1140/epjd/e2007-00227-1

THE EUROPEAN PHYSICAL JOURNAL D

Mode hopping strongly affects observability of dynamical instability in optical parametric oscillators

A. Amon[1,a] and M. Lefranc[2]

[1] Laboratoire PALMS, UMR CNRS 6627, Université de Rennes I, Campus de Beaulieu, 35042 Rennes Cedex, France
[2] Laboratoire PhLAM, UMR CNRS 8523, CERLA, Université des Sciences et Technologies de Lille, 59655 Villeneuve d'Ascq Cedex, France

Received 30 January 2007 / Received in final form 29 May 2007
Published online 29 June 2007 –

Abstract. Theoretical investigations of dynamical behavior in optical parametric oscillators (OPO) have generally assumed that the cavity detunings of the interacting fields are controllable parameters. However, OPOs are known to experience mode hops, where the system jumps to the mode of lowest cavity detuning. We note that this phenomenon significantly limits the range of accessible detunings and thus may prevent instabilities predicted to occur above a minimum detuning from being evidenced experimentally. As a simple example among a number of instability mechanisms possibly affected by this limitation, we discuss the Hopf bifurcation leading to periodic behavior in the monomode mean-field model of a triply resonant OPO and show that it probably can be observed only in very specific setups.

PACS. 42.65.-k Nonlinear optics – 42.65.Sf Dynamics of nonlinear optical systems; optical instabilities, optical chaos and complexity, and optical spatio-temporal dynamics – 42.65.Yj Optical parametric oscillators and amplifiers

1 Introduction

Continuous-wave optical parametric oscillators (OPOs) are tunable sources of coherent light that have proved extremely useful in quantum optics or high resolution spectroscopy [1]. They also have attracted great interest as model systems in nonlinear dynamics because they are based on the simplest optical nonlinearity, three-wave mixing, and are expected to exhibit complex dynamical behavior in some regions of parameter space. Indeed, many theoretical studies have predicted a variety of complex temporal and spatio-temporal dynamics (see, e.g., [2–10]). In particular, the simplest model of a triply resonant OPO (TROPO), the degenerate monomode mean-field model, was shown twenty-five years ago to display a Hopf bifurcation leading to periodic behavior [2,3], and later to exhibit deterministic chaos [4]. Quite surprisingly, this instability has to our knowledge not yet been observed experimentally. Although oscillatory behaviors have been reported in several experiments [11–14], they have been shown to stem either from thermal effects [12,13] or from the interaction of transverse modes [14]. Very recently, chaotic behavior has been evidenced in a TROPO [15] but is believed to be also linked to multimode operation.

The most important control parameters controlling the appearance of instabilities in OPOs are probably the pumping rate and the cavity detunings. Indeed, a higher pumping rate implies stronger nonlinearities and non-zero detunings increase the effective number of dynamical variables. As a matter of fact, most instabilities investigated theoretically have usually been described at large values of the pumping rate and for cavity detunings significantly above zero (for example, several numerical simulations of pattern-forming instabilities shown in [5–9] use signal detuning values slightly or well above the cavity resonance half-width).

As pumping rate is obviously limited by the power of the pump laser, it would only be natural to identify it as the limiting factor when searching for instabilities [10]. As for detunings, they are generally considered as parameters that can be easily tuned so as to pull the system away from equilibrium and observe complex behaviors. However, there are two limitations on the values that cavity detunings can take. The first is simply that the OPO threshold increases quadratically with detuning, and thus that operation is restricted to detuning values for which threshold power remains below available pump power. The second arises because of a phenomenon known as mode hopping: OPOs spontaneously choose their operation frequency so as to operate on the cavity mode with smallest detuning. As the OPO is pulled away from a cavity resonance in order to increase detuning, a more favorable operating point appears near another cavity resonance and the

[a] e-mail: axelle.amon@univ-rennes1.fr

system jumps to it. Because mode hops in OPOs occur for variations of cavity length as small as a few nanometers, they make it difficult to stabilize doubly or triply resonant OPO and to achieve smooth tuning [16–19]. Here, our concern is that mode hops prevent the OPO from achieving high values of the detunings and thus restraint the parameter range that can be explored. Such a limitation might very well preclude the experimental observation of dynamical behaviors predicted theoretically.

In this paper, we discuss this problem in a simple example, the Hopf bifurcation that leads to periodic behavior in the monomode mean-field model of a TROPO. We show that mode selection in OPOs indeed prevents experimental observation of this instability in most practicable configurations. We first recall the basic properties of the monomode mean-field TROPO model and the conditions under which the Hopf bifurcation occurs. In the limit of infinite pump power, a simple lower bound for signal detunings at which the Hopf bifurcation can occur is easily obtained, which confirms that this bifurcation requires high values of the signal detuning. In a second part we derive the expression of the maximal value that signal detuning can reach before a mode hop occurs, which depends on the length and finesse of the cavity as well as on crystal birefringence. By comparing the two bounds and searching for parameter regions where they are compatible, we find that mode hops generally keep the TROPO away from parameter ranges where the Hopf bifurcation can be observed, unless very high-finesse and very short cavities are used, which would make operation extremely difficult. This is confirmed by a numerical exploration at finite pump power of the parameter space of this model for various values of the cavity finesse. It shows that mode hopping rather than pump power is the limiting factor in order to reach instability. This result provides a plausible explanation of the fact that the Hopf bifurcation of the monomode TROPO has not yet been observed experimentally. It also calls for further investigations in order to determine whether mode hopping also interferes with other predicted instabilities.

2 TROPO degenerate monomode mean-field model: Hopf instability

We now recall the main features of the simplest TROPO model, the degenerate longitudinally and transversely monomode mean-field model [2–4]. Light generation in an optical parametric oscillator is based on parametric down-conversion in a nonlinear crystal of a pump photon into two lower-frequency photons called signal and idler. In a TROPO, the optical cavity enclosing the crystal is resonant for all three fields so as to minimize operation threshold. In the mean-field (a.k.a. uniform-field) approximation, the time evolution of the normalized amplitudes A_s, A_i and A_p of the signal, idler and pump fields inside the cavity can be described by the following differential equations [4]:

$$\dot{A}_s = -(1 + i\Delta_s)A_s + A_i^* A_p, \tag{1a}$$

$$\dot{A}_i = -(1 + i\Delta_i)A_i + A_s^* A_p, \tag{1b}$$

$$\dot{A}_p = \gamma\left[-(1 + i\Delta_p)A_p - A_s A_i + E\right], \tag{1c}$$

where Δ_s, Δ_i and Δ_p are the detunings between the optical frequency and the frequency of the closest cavity resonance for the signal, idler and pump fields, respectively, and E is the pumping rate. The time unit is the cavity decay time of the signal field and γ is the cavity decay rate for the pump. In this paper we focus on the stationary regimes of equations (1), and are interested in determining when they become unstable to give birth to periodic oscillations depending on values of control parameters.

A little known property of equations (1) is that although the signal and idler fields are in principle distinct, their time evolution can be described by a single amplitude after transients have died out. First it should be noted that stationary solutions of equations (1) exist only for $\Delta_s = \Delta_i$, a relation that can be shown to follow from photon number conservation [20]. Replicating a similar calculation carried out in the analysis of a bimode model [21], it is then easy to show that equations (1a) and (1b) imply that after a sufficiently long time, the amplitudes A_s and A_i are equal up to a constant phase difference that can always be removed by a redefinition of the amplitudes. This is obviously linked to the fact that signal and idler photons are twin photons created in the same quantum process. Without loss of generality, the asymptotic dynamics of the TROPO can then be modeled by the following normalized equations (degenerate model) describing the time evolution of the complex amplitude of the signal field A_s and of the pump field A_p [4]:

$$\dot{A}_s = -(1 + i\Delta_s)A_s + A_s^* A_p, \tag{2a}$$

$$\dot{A}_p = \gamma\left[-(1 + i\Delta_p)A_p - A_s^2 + E\right]. \tag{2b}$$

For pumping rates above the parametric emission threshold given by

$$E_{th}^2 = (1 + \Delta_p^2)(1 + \Delta_s^2), \tag{3}$$

equations (2) have non-zero stationary solutions which have been shown to fit accurately experimental observations in the vicinity of threshold [11]. When pump rate is increased, these stationary solutions can become unstable through a Hopf bifurcation giving rise to oscillatory behavior [2–4]. A necessary condition for this bifurcation is [4]

$$\Delta_p \Delta_s < -\left[1 + \frac{\gamma(1 + \Delta_p^2)}{2}\right], \tag{4}$$

which ensures that there is a finite pump rate $E_H > E_{th}$ at which the stationary nonzero solution bifurcates to a periodic solution, which is is given by [4]

$$E_H^2 = \left[\frac{\gamma^2(1 + \Delta_p^2) + 4(1 + \gamma)}{-2(1 + \gamma)^2[1 + \frac{2(1+\Delta_p\Delta_s)}{\gamma(1+\Delta_p^2)}]} - (\Delta_p\Delta_s - 1)\right]^2 + (\Delta_p + \Delta_s)^2, \tag{5}$$

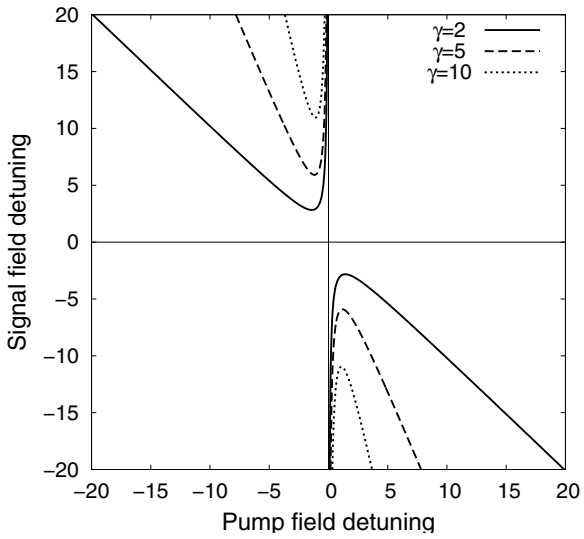

Fig. 1. Map (Δ_p, Δ_s) for different values of the parameter γ. The curves delimits the areas for which condition (4) is fulfilled.

At higher pump rates, the limit cycle born in the Hopf bifurcation undergoes a period-doubling cascade leading to chaos [4].

As inequality (4) is closer and closer to equality, the Hopf threshold E_H given by (5) becomes larger and larger and is eventually rejected to infinity. For a given maximal pump rate available, $E_{\max}$, whether the instability can be observed at fixed detunings inside the parameter domain delimited by (4) is determined by the inequality $E_{\max} > E_H(\Delta_p, \Delta_s)$. Since we are interested here in specifying the unstable region by simple bounds on the detunings, we first assume that we have infinite pump power available. Under this approximation, whose validity will be checked in numerical simulations in Section 4, the Hopf instability domain is solely determined by inequality (4).

The instability domains in the (Δ_p, Δ_s) plane have been plotted in Figure 1 for different values of γ, and are seen to be bounded away from the origin. Along their boundaries, (4) is an equality and defines the signal detuning as a function of pump detuning. It is easily found that the minimum absolute value that the signal detuning can take on the boundary, and hence in the instability domain, is:

$$\Delta^H_{\min} = \min\{|\Delta_s|\} = \sqrt{\gamma(\gamma+2)}, \tag{6}$$

and is obtained for $|\Delta_p| = \sqrt{(2+\gamma)/\gamma}$. Note that $\Delta^H_{\min}$ is roughly proportional to γ and thus increases with it.

Since (4) still holds at finite pump power, the lower bound provided by (6) is always valid. This clearly shows that the Hopf bifurcation of the monomode degenerate mean-field model can only occur for sufficiently high signal detunings. In the next section, we describe the process of mode hopping and how it limits the values that signal detunings can take leading to a maximal absolute value for the detunings. Whether the two constraints can be satisfied simultaneously will eventually determine whether the Hopf bifurcation can be observed experimentally.

3 Limitation of signal detuning due to mode hopping

3.1 Theory

In the theoretical analysis of Section 2, it was assumed that the frequency detuning of the signal field is a fixed parameter. This is however not entirely true, because the operating frequency of an OPO is not actually chosen by the experimentalist but results from a complex mode selection process. While small variations of the cavity length most often modify frequency and hence detuning gradually, sudden jumps will occur when a remote operating point becomes more favorable. As we discuss below, this process tends to minimize frequency detuning and consequently to limit its maximum value, which can be derived analytically.

As with any optical oscillator where an amplifying medium is enclosed inside an optical cavity, there are two main constraints that determine the operating conditions of an OPO: the first one is that the gain in the amplifying medium must be sufficient to overcome cavity losses over each round trip in the cavity, the second one is that the generated field must be nearly resonant with one of the cavity modes so that amplification by the gain medium is cumulative over successive round trips.

In optical parametric oscillators, the nonlinear interaction is optimal when the relative phases of the three interacting waves remain fixed during propagation. The phase-matching condition is easily formulated in a corpuscular point of view: the conversion of one pump photon into signal and idler photons must satisfy energy and momentum conservation:

$$\omega_p = \omega_s + \omega_i \tag{7a}$$

$$\boldsymbol{k}_p = \boldsymbol{k}_s + \boldsymbol{k}_i \tag{7b}$$

where $\omega_{p,s,i}$ and $k_{p,s,i}$ denote the frequencies and the wavevectors of the pump, signal and idler fields.

The pump properties being fixed, relations (7) generally single out unique values for the signal and idler frequencies and much of OPO design consists in ensuring that these values fall in the desired frequency range. However, while energy conservation (7a) strictly holds for continuous-wave OPOs, momentum conservation may be satisfied only approximately because of the finite size of the nonlinear crystal. Thus there is a small but finite frequency domain around the exact phase-matching frequency where the nonlinear gain is adequate for OPO operation. It is usually the case that many cavity resonances fall inside this domain, and an important problem is to determine the resonances near which oscillation will actually occur.

Monomode optical parametric oscillators behave as homogeneously broadened lasers in that when there are several frequencies for which gain overcome losses in the empty cavity, the one with the lowest threshold takes over by saturating the gain in such a way that competing modes remain below threshold. Mode selection thus amounts to

determining which operating modes have lowest threshold. If variation of raw gain in the domain around perfect phase-matching is neglected, and considering pump detuning as a fixed parameter, this is equivalent to finding the allowed operating frequencies for signal and idler fields that have lowest frequency detuning, as expression (3) for parametric threshold shows.

In doubly and triply resonant OPOs, this problem is made difficult by the fact that the signal and idler fields must be simultaneously resonant. Thus operation can only take place at coincidences between two frequency combs. In general the two combs have different periods, either because the signal and idler fields have very different frequencies or because they are polarized along different axes of a birefringent crystal (the so-called type-II phase-matching [22]). A singular configuration that we will not consider here is when signal and idler have identical polarizations and frequencies (type-I phase matching at degeneracy). As a result, frequency tuning in OPOs is a complicated problem that has been studied very carefully both in the type-I and type-II cases [16,17].

The detunings of the signal and the idler fields are given respectively by $\Delta\omega_s = \omega_s - \omega_s^R$ and $\Delta\omega_i = \omega_i - \omega_i^R$, where ω_s and ω_i are the optical frequencies of the signal and idler fields and ω_s^R and ω_i^R are the closest resonance frequencies of the cavity. For the sake of simplicity, we assume in the following that ω_s and ω_i are close to a 1:1 ratio but the argument can be generalized easily to any rational number.

Taking energy conservation (7a) into account, the total frequency mismatch $\Delta\omega = \Delta\omega_s + \Delta\omega_i$ for the signal-idler mode pair is given by:

$$\Delta\omega = \omega_p - \omega_s^R - \omega_i^R, \tag{8}$$

which does not depend of the specific oscillation frequencies ω_s and ω_i chosen by the system, but only of the pump frequency and the resonance frequencies of the cavity for the signal and the idler modes. For our purposes, $\Delta\omega$ is the relevant quantity to consider as the individual detunings $\Delta\omega_s$ and $\Delta\omega_i$ are proportional to it in a stationary state, as a consequence of energy and photon number conservation [20]. The mode pair selected by the OPO will be the one that minimizes the total frequency mismatch $\Delta\omega$ so as to minimize threshold.

Taking into account that ω_s^R and ω_i^R belong to two frequency combs specified by the free spectral ranges $\delta\omega_s$ and $\delta\omega_i$:

$$\omega_s^R = N_s\delta\omega_s, \quad \omega_i^R = N_i\delta\omega_i \tag{9}$$

where N_s and N_i are the mode indices, and having in mind that $|\delta\omega_s - \delta\omega_i| \ll \delta\omega_s, \delta\omega_i$, we rewrite (8) as

$$\Delta\omega = \omega_p - \bar{N}(\delta\omega_s + \delta\omega_i) - \Delta N(\delta\omega_s - \delta\omega_i) \tag{10}$$

with $\bar{N} = (N_s + N_i)/2$ and $\Delta N = (N_s - N_i)/2$. Under our hypotheses, we have $\Delta N \ll \bar{N}$. Hence the last term in (10) is in first approximation negligible compared to the second term, and the integer value of $\bar{N}$ that minimizes $\Delta\omega$ is determined independently of ΔN. Then the optimization problem can be refined by searching for the integer value of ΔN that minimizes (10) at fixed $\bar{N}$. Studies of tuning properties of double or triply resonant OPO have shown that the operating modes are grouped into clusters, each cluster consisting of a sequence of adjacent modes [16,17]. In (10), $\bar{N}$ indicates the cluster and ΔN distinguishes between adjacent modes inside the cluster.

An important consequence of (10) is that $\Delta\omega$ can at best be adjusted in steps of $|\delta\omega_s - \delta\omega_i|$. With such steps, the frequency mismatch $\Delta\omega$ can always be made to belong to the interval $[-\frac{|\delta\omega_s-\delta\omega_i|}{2}, \frac{|\delta\omega_s-\delta\omega_i|}{2}]$ but cannot be brought closer to zero. This minimal $\Delta\omega$ corresponds to the mode pair chosen by the OPO. By considering the worst case, the maximal frequency mismatch that can be reached is

$$\Delta\omega_{\max} = \frac{|\delta\omega_s - \delta\omega_i|}{2}, \tag{11}$$

which agrees with the general expression of the detuning given in [16]. As the OPO is pulled away from an exact cavity resonance by increasing the cavity length, the frequency mismatch will increase up to the maximal value given by (11), at which point there will be an operating mode with a lower mismatch to which the OPO will switch. This phenomenon is well known as mode hopping [16,17].

Before (11) can be compared with the bound found for the Hopf bifurcation in Section 2, it has to be expressed in the same units. The detunings used in equations (2) are normalized so that half-height width of the cavity resonance is 2. Since the cavity finesse $\mathcal{F}$ is defined so that the half-height width is $\delta\omega/\mathcal{F}$, we have

$$\Delta_s = 2\mathcal{F}_s\frac{\Delta\omega_s}{\delta\omega_s}, \tag{12a}$$

$$\Delta_i = 2\mathcal{F}_i\frac{\Delta\omega_i}{\delta\omega_i}. \tag{12b}$$

As mentioned before, Δ_s and Δ_i are not independent in the stationary regime but obey the simple relation $\Delta_s = \Delta_i$ as a consequence of energy and photon number conservation [20]. Taking into account that $\Delta\omega = \Delta\omega_s + \Delta\omega_i$, one obtains from (12):

$$\Delta_s = \Delta_i = \frac{2\mathcal{F}_s\mathcal{F}_i\Delta\omega}{\mathcal{F}_i\delta\omega_s + \mathcal{F}_s\delta\omega_i}. \tag{13}$$

This expression was derived assuming $\omega_s \simeq \omega_i$, so that we should fix $\mathcal{F}_s \simeq \mathcal{F}_i$ for consistency. The maximal value of the frequency mismatch authorized by mode selection, as given by equation (11), can thus be rewritten as

$$\Delta^M_{\max} = \mathcal{F}_s\frac{|\delta\omega_s - \delta\omega_i|}{\delta\omega_s + \delta\omega_i}. \tag{14}$$

Before we can discuss whether the Hopf bifurcation can be observed in typical experiments, we have to reformulate (14) in terms of the experimental configuration.

Given that

$$\delta\omega_{s,i} = \frac{2\pi c}{2(L_{cav} + (n_{s,i} - 1)l_c)} \tag{15}$$

where L_{cav} is the geometric length of the cavity, l_c is the length of the nonlinear crystal, $n_{s,i}$ the indices of the signal (resp. idler) fields and c is the celerity of light in the vacuum, (14) can be rewritten as

$$\Delta^M_{\max} = 2\mathcal{F}_s \frac{|\delta n| l_c}{[L]}, \tag{16}$$

where

$$[L] = 2\left(L_{cav} + \left(\frac{n_s + n_i}{2} - 1\right) l_c\right)$$

is the average optical path for the signal and the idler fields over one round trip in the cavity and

$$\delta n = \frac{|n_s - n_i|}{2}.$$

In the limit case of a monolithic OPO ($L_{cav} = l_c$), expression (16) leads to the remarkably simple expression

$$\Delta^M_{\max}/\mathcal{F}_s = \frac{2|\delta n|}{n_s + n_i} \tag{17}$$

showing the key role played by crystal birefringence. Expression (17) yields an absolute upper bound for (16) since cavity length obviously cannot be smaller than crystal length.

Note that since $\delta n \ll n_{s,i}$ for a standard crystal, expressions (16) and (17) ensure that the small-detuning hypothesis of the mean-field approximation is fulfilled for the signal and idler fields.

We are now in a position to obtain a simple criterion to determine whether the Hopf bifurcation can be observed in a given configuration at infinite pump power. Obviously, we must have

$$\Delta^H_{\min} < \Delta^M_{\max} \tag{18}$$

which, using (6) and (16), and expressing the pump cavity decay rate as

$$\gamma = \frac{\mathcal{F}_s}{\mathcal{F}_p},$$

translates into

$$\sqrt{\frac{1}{\mathcal{F}_p}\left(\frac{1}{\mathcal{F}_p} + \frac{2}{\mathcal{F}_s}\right)} < 2\frac{|\delta n| l_c}{[L]} \tag{19}$$

which is the main result of our paper. Again, (19) simplifies in the monolithic case. A noteworthy feature of inequality (19) is the asymmetry in the dependences with respect to the pump and signal finesse. It is easily seen that increasing pump finesse is much more effective to have (19) satisfied. Assuming $\mathcal{F}_p = 50$ and $\mathcal{F}_s = 500$, doubling the pump finesse decreases the left hand side of (19) by 46% while doubling the signal finesse only does so by 4%.

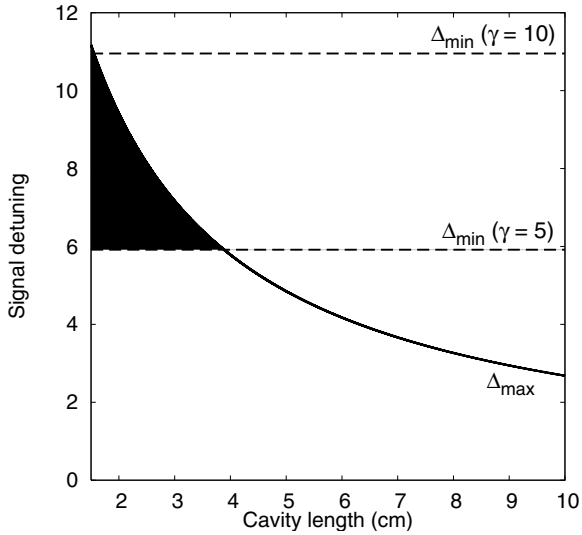

Fig. 2. Solid lines: values of maximal detuning authorized by mode selection when cavity length is varied between 1.5 cm and 10 cm. Dashed lines: minimal detuning permitted by the conditions of the Hopf bifurcation for two different values of γ: 5 and 10.

3.2 Numerical estimates

To get a better understanding of whether the criterion obtained in Section 3.1 is easily satisfied or not, we now compute numerical estimates for typical experimental configurations. In previous experiments [12–15,21], we used a KTP crystal of length $l_c = 15$ mm cut for type-II phase-matching, with an extraordinary index $n_e = 1.75$ and an ordinary index $n_o = 1.83$. The crystal is enclosed in a Fabry-Perot cavity delimited by two spherical mirrors with a radius of curvature of 5 cm. The cavity finesse for the signal and pump fields are around 500 and 50, respectively.

The most easily adjustable parameter is the geometrical cavity length, which is bounded from below by the crystal length (1.5 cm) and from above by the concentric condition ($\sim$10 cm). Figure 2 shows the evolution of the maximal detuning $\Delta^M_{\max}$ with cavity length. The main feature is that $\Delta^M_{\max}$ decreases monotonically with cavity length, as is easily seen in expression (16). Thus the most favorable situation will always be obtained in the "monolithic" configuration where cavity length equals crystal length. In practice, this configuration cannot be reached when spherical mirrors are used because of the size of the crystal mount, but the shortest feasible cavity length (3 cm in our experiments) should be sought.

In our experiment, $\gamma = \mathcal{F}_s/\mathcal{F}_p = 10$, from which we can compute the value $\Delta^H_{\min} = \sqrt{\gamma(\gamma+2)}$ of the minimal detuning necessary to obtain the Hopf bifurcation. This value does not depend on cavity length and is represented in Figure 2 by the upper dashed horizontal line. We see that there is hardly a configuration where $\Delta^H_{\min} < \Delta^M_{\max}$. In this configuration, the Hopf bifurcation cannot be observed regardless of pump power because mode hopping prevents to reach sufficiently high detunings.

In order to lower $\Delta_{\min}^{H}$, assume now that pump finesse is increased to 100 so that γ decreases to 5. This corresponds to the lower horizontal dashed line in Figure 2. There is now a range of cavity lengths where $\Delta_{\min}^{H} < \Delta_{\max}^{M}$ as shown by the black area between the two curves.

If $\mathcal{F}_s$ and $\mathcal{F}_p$ are increased simultaneously keeping γ constant, $\Delta_{\max}^{M}$ will increase while $\Delta_{\min}^{H}$ remains unchanged, and the instability region will also widen.

3.3 Conclusion

In this section we have taken into account the fact that the signal frequency detuning is not a fixed parameter but is determined by the operating frequency chosen by the OPO so as to minimize this detuning. As a result the signal frequency detuning is bounded from above by the mode hopping phenomenon. Since signal detunings at which periodic behaviors appear are bounded from below, the Hopf bifurcation can only be observed if $\Delta_{\min}^{H} < \Delta_{\max}^{M}$. Our analysis has shown that even in the ideal case where infinite pump power is available, mode hopping can prevent from reaching detunings sufficiently large to observe the Hopf bifurcation of the monomode model.

The numerical estimates obtained for the configuration used in our previous experiments explain why we could not observe the Hopf bifurcation in this setup. In order to obtain instabilities, one should take into account that $\Delta_{\min}^{H}$ depends on the ratio of signal and pump finesse while $\Delta_{\max}^{M}$ is proportional to signal finesse. More generally, the finesse should satisfy inequality (19). As will be discussed in Section 5, the theoretically most favorable configurations are extremely difficult to build experimentally. In all cases, cavity should be made as short as possible.

It remains to be checked that in cases where the instability can be observed, it persists when pump power is limited. We do so in Section 4.

4 Numerical investigations at finite pump power

So far, our analysis has assumed infinite pump power, which has allowed us to obtain simple analytical formulas such as (19) to decide whether the Hopf bifurcation is screened by mode hopping or not. We now have to determine how good this approximation is in the real-life situation where only finite pump power is available and if conclusions drawn from our theoretical analysis remain relevant.

At finite pump power, whether the Hopf bifurcation can be observed no longer depends only on inequality (4) but also on whether the Hopf threshold (5) can be reached given available pump power. Because expression (5) is much more complicated than inequality (4), we restrict ourselves here to a numerical exploration of the detuning ranges where periodic behavior is found and compare our results with predictions from the infinite pump power analysis. This exploration is carried out for several values of the cavity finesse, other parameters being chosen so as to match our previous experiments [12–15,21]. As we shall see, it will allow us to conclude that pump power is not a limiting factor with commonly available pump lasers and that the criteria derived in the infinite pump power analysis remain relevant.

A few general observations are in order before we present our numerical results. The relevant criterion is whether the minimum detuning $\Delta_{\min}^{H}$ at which Hopf bifurcation occurs is smaller than the larger detuning $\Delta_{\max}^{M}$ allowed by mode hopping. Thus it is interesting to comment on how these bounds evolve when pump power is limited.

Regarding onset of periodic behavior, it should be recalled that inequality (4) holds regardless of pump power, that equality can be achieved only for infinite pump power and that otherwise the Hopf threshold (5) yields a more stringent condition than (4) on the detunings. As a result, the instability regions are systematically shifted towards higher values of the detunings, leading to an increase of $\Delta_{\min}^{H}$ compared to expression (6).

As for the maximal value $\Delta_{\max}^{M}$ of the detuning allowed by mode hopping [Eq. (14)], it does not depend on pump power as it is obtained by considering the frequency combs of the cavity resonances. However a limitation that has to be taken into account at finite pump power is that if the OPO is below parametric emission threshold at $\Delta_s = \Delta_{\max}^{M}$, then the latter bound certainly cannot be achieved and the actual bound will be lower (the stationary ON state must exist for the bifurcation to occur). Using the expression for parametric threshold (3), the expression for the maximal signal detuning value becomes

$$\Delta_{\max}^{MT} = \min\left(\Delta_{\max}^{M}, \sqrt{\frac{E^2}{1+\Delta_p^2} - 1}\right) \qquad (20)$$

where E is the pump parameter and Δ_p is the pump detuning. The compatibility between the values of the minimal detuning at which periodic behavior occurs and of the maximal detuning at which stationary parametric emission occurs is now more difficult to analyze because both depend on pump detuning. However, it is easy to see that as pump power is decreased, the former can only increase and the latter only decrease so that the Hopf bifurcation is necessarily harder to observe in the finite pump power case. We now assess by how much by carrying out numerical simulations.

The phase diagrams in Figure 3 shows in black the regions in the (Δ_p, Δ_s) parameter plane where periodic behavior is found for different values of the cavity finesse, the values of the remaining parameters being fixed so as to match our experiments [12–15,21]. For each parameter set, the dynamical regime is classified as periodic when

- inequality (4) is satisfied, and
- $E_H(\Delta_p, \Delta_s) < E_{max}(\mathcal{F}_p, \mathcal{F}_s)$

where $E_{\max}(\mathcal{F}_p, \mathcal{F}_s)$ is the maximum pump parameter corresponding to the pump power available in our

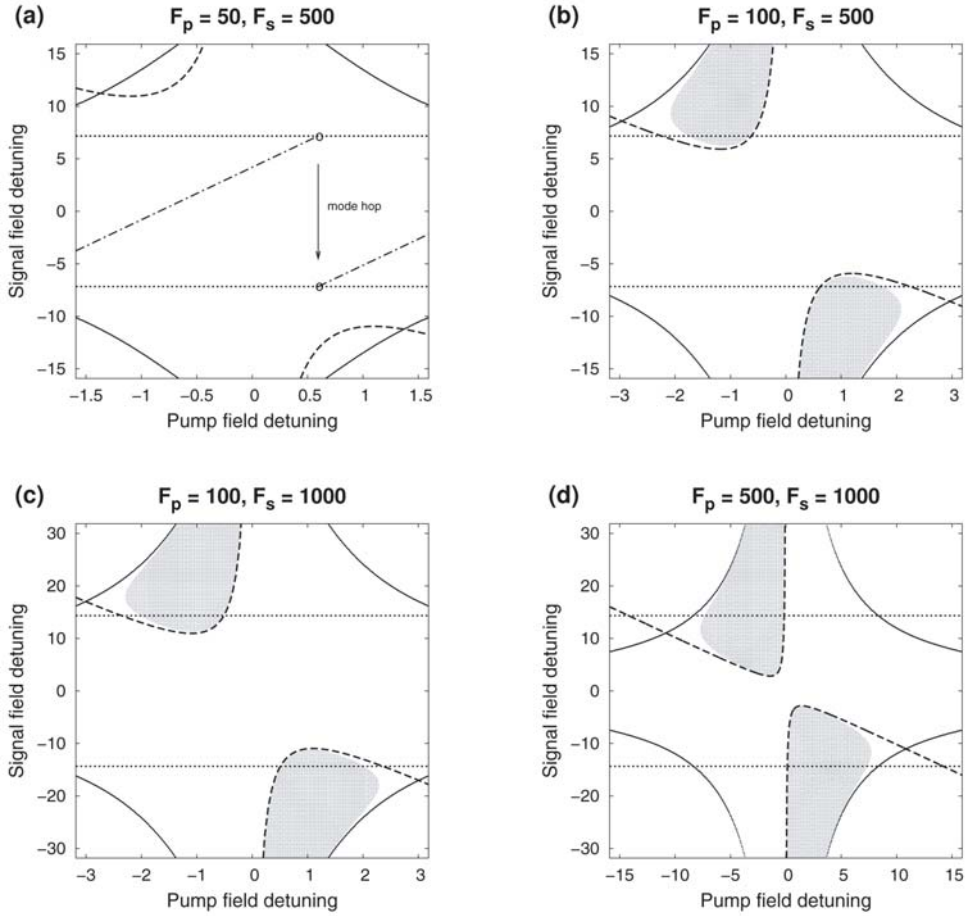

Fig. 3. Phase diagrams in the (Δ_p, Δ_s) plane showing the instability regions as black areas for different values of the finesse of the pump ($\mathcal{F}_p$) and of the signal ($\mathcal{F}_s$) field: (a) $\mathcal{F}_p = 50$, $\mathcal{F}_s = 500$, (b) $\mathcal{F}_p = 100$, $\mathcal{F}_s = 500$, (c) $\mathcal{F}_p = 100$, $\mathcal{F}_s = 1000$, (d) $\mathcal{F}_p = 500$, $\mathcal{F}_s = 1000$. Solid curves delimit areas above parametric emission threshold. Dashed lines indicate where (4) is an equality and delimit unstable areas in the infinite pump power approximation. Dotted horizontal lines indicate the maximal detuning value allowed by mode hops. In (a), the dotted and dashed line shows a possible path followed by detunings as cavity length is scanned. The discontinuity occurring as the path reaches the horizontal dotted line corresponds to a mode hop.

experimental conditions (4 W)[1]. Since the unstable zones are enclosed inside the regions where parametric emission occur and the instability regions at infinite pump power, the boundaries of these regions, which can be computed analytically, are also shown in Figure 3 so that we can estimate how well they approximate the numerical results. In order to make meaningful comparisons between setups corresponding to different values of the finesse, the domains of variations of the pump and signal detunings are chosen so that $\Delta_{s,p} \in [-\mathcal{F}_{s,p}/(10\pi), \mathcal{F}_{s,p}/(10\pi)]$. This corresponds in each case to the same variation of the physical cavity length ($\Delta L = \lambda/40\pi$) and thus there is no difference in the scans from an experimental point of view. Since $|\Delta_{s,p}| \ll 2\mathcal{F}_{s,p}$, this also ensures that the small-detuning hypothesis of the mean-field model is satisfied.

Figure 3a shows that for parameter values corresponding to our experimental setup, periodic behavior does not occur, explaining why we do not observe the Hopf bifurcation in this setup. It also shows that the boundaries of the unstable region at infinite pump power are located outside the central band where $\Delta_s \in [-\Delta^M_{\max}, \Delta^M_{\max}]$ and thus that mode hopping prevents the bifurcation from being observed in this configuration even if infinite pump power was available. The proximity of the two curves corresponding to parametric threshold and bifurcation at infinite pump power probably explains why no instability can be observed.

In contrast with Figure 3a, Figures 3b to 3d display larger and larger instability zones as cavity finesse are increased. While in Figure 3b the intersection of the unstable region with the central band of allowed signal detunings is very small, it becomes sizable in Figure 3d. More precisely, the fraction of the central band occupied by unstable regions is 1.6% in Figure 3b, 3.5% in Figure 3c and 17% in Figure 3d. These numbers are meaningful as probability estimates if we assume that there is no correlation between the signal and pump detunings on average, i.e., that the entire allowed band may be explored over several experiments. It should be noted that during a scan of cavity length through a single resonance of the pump, pump and signal detuning will vary jointly as illustrated in Figure 3a and that this may affect the probability of hitting the unstable zone. However, it is expected that there is no relation between paths followed in the (Δ_p, Δ_s) plane for different pump resonances so that no part of the allowed band should remain inaccessible.

[1] $E_{max}(\mathcal{F}_p, \mathcal{F}_s) = \sqrt{\mathcal{P}_{max}/\mathcal{P}_{th}(\mathcal{F}_p, \mathcal{F}_s)}$ with $\mathcal{P}_{max}$ the maximum pump power available and $\mathcal{P}_{th}(\mathcal{F}_p, \mathcal{F}_s)$ the pump power at threshold. It is known that $\gamma_p \mathcal{P}_{th}(\mathcal{F}_p, \mathcal{F}_s) \propto \gamma_s^2 \gamma_p^2$ [17, 23] and consequently $\frac{E^2_{max}(\mathcal{F}_p, \mathcal{F}_s)}{\mathcal{F}_p \mathcal{F}_s^2} = cst.$ In our experimental setup, $\mathcal{F}_{p0} = 45$, $\mathcal{F}_{s0} = 550$, $\mathcal{P}_{max} \simeq 4$ W and $\mathcal{P}_{th}(\mathcal{F}_{p0}, \mathcal{F}_{s0}) \simeq 10$ mW, which leads to $\frac{E^2_{max}(\mathcal{F}_p, \mathcal{F}_s)}{\mathcal{F}_p \mathcal{F}_s^2} \simeq 400$.

Examination of Figures 3a–3d shows that although increasing finesse globally makes it easier to observe the Hopf bifurcation, finesse for the pump and signal fields have different influences. The twofold increase in $\mathcal{F}_p$ between Figures 3a and 3b clearly modifies the phase diagram much more than the twofold increase in $\mathcal{F}_s$ between Figures 3b and 3c. Similarly, increasing $\mathcal{F}_p$ from 100 to 500 is critical to have a significant probability of observing the Hopf bifurcation. This is consistent with the discussion of criterion (19) in Section 3 which showed that increasing pump finesse was much more effective than increasing signal finesse. However increasing pump finesse is extremely difficult from a practical point of view, as we discuss in Section 5. Interestingly, it was similarly noted in reference [10] that increasing pump finesse while keeping signal finesse allowed one to observe an hexagonal transverse pattern at lower signal detunings.

An important conclusion that can be drawn from the numerical exploration summarized in Figures 3a–3d is that except in Figure 3a, the theoretical analysis at infinite pump power provides a very good approximation of the finite pump power case, all the better as finesse are higher and as observing the Hopf bifurcation becomes more plausible. Indeed the instability zones are tightly delimited by the boundaries obtained at infinite pump power and by the parametric threshold line except for larger pump detunings. In particular, the agreement is excellent at the tip of the unstable zones, near the point of minimal signal detuning. This makes us confident that for pump lasers currently available, the criterion obtained in (19) is effective in assessing the probability of occurrence of the Hopf bifurcation. It also shows that pump power is not a limiting factor as when there is a nonempty intersection between the unstable zone and the central band of allowed detunings, its area only marginally increases from the finite to the infinite pump case, mostly in regions far from the minimum detuning value.

To conclude, numerical calculations at finite pump power show that while the Hopf bifurcation becomes harder to observe than in the infinite pump power case, the mode hopping phenomenon remains the main limiting factor by limiting the range of values signal detuning can take. In order to obtain experimental evidence of the bifurcation, building a dedicated setup would be much more effective than increasing pump power. However, there are some experimental difficulties in doing so, which we discuss in Section 5.

5 Experimental considerations

The theoretical analysis at infinite pump power of Section 3 and the numerical computations at finite pump power of Section 4 have suggested that the Hopf bifurcations of the monomode mean-field model might be observable in some configurations. In this section, we discuss the feasibility of an experimental setup specially designed for evidencing the bifurcation.

Some parameters are easily optimized using the findings of Sections 3 and 4. As discussed in Section 3.2, cavity should be as short as possible and in this respect a monolithic configuration would be optimal. Then, crystal birefringence should be chosen as large as possible [see Eq. (17)]. However this may not be an option as brifrigence is primarily used to achieve phase-matching in the desired operating range. Of course, pump power should be as large as possible, but our analysis has shown that there were modest returns in increasing it much beyond that offered by currently available pump lasers. The two parameters left for setup optimization are then the signal and pump cavity finesse. Criterion (19) indicates that those finesse, and especially the pump finesse, should be taken as large as possible.

However, cavities of very high finesse are critical to align and are very sensitive to fluctuations. For example, a change of δL of the cavity length will induce a variation of $\delta\Delta = 4\mathcal{F}\delta L/\lambda$ of the detuning, where λ is the optical wavelength. For $\lambda = 1064$ nm and $\mathcal{F} = 1000$, a fluctuation $\delta L = 5$ Å of the cavity length will induce a variation of the detuning $\delta\Delta = 2$, corresponding to full-width of the resonance. The length of the cavity must thus be adjusted carefully and maintained constant to within less than a few angströms.

This stability problem is all the more critical when thermal effects are taken into account. In our configuration, it has been shown that thermal effects can induced complex dynamical behaviors [12,13] during which cavity length can be spontaneously swept by a few nanometers. Such instabilities were observed even at incident pump powers around 500 mW [12], which for a pump finesse of 45 corresponds to an intracavity pump power of about 6.5 W. For 4 W of incident pump power and a finesse of 500, intracavity pump power would reach ∼640 W at resonance and thermal effects would then be a hundred times as strong. For illustration purposes, let us recall that the only chaotic regime reported so far in an TROPO was observed in a situation where cavity length could not be made stationary [15], although the configuration was standard.

Another adverse influence of pump absorption in the crystal is that it puts a limit on the highest finesse achievable. In our setup, for example, pump absorbtion in the 1.5 cm-long crystal is 2% cm^{-1} which implies that pump finesse cannot be higher than about 100 even if perfectly reflecting mirrors were used. Except for crystals with exceptional low absorption, high values of the pump cavity finesse such as 500 appear to be completely unrealistic.

Apart from the previous remarks which hold for all systems featuring an absorbing material enclosed in a resonant cavity, specific restrictions on the finesse are to be considered for a TROPO, inside which several fields must be simultaneously resonant. Generally cavity finesse in an experimental TROPO setup are chosen so that $\mathcal{F}_p \ll \mathcal{F}_s$. It ensures that numerous resonances of the signal field are found inside the wider resonance of the pump field, in other terms that several mode hops occur before OPO falls below threshold. This allows one to only consider coincidences of signal and idler cavity modes. For very high cavity finesse of the pump, the mode with smallest signal

detuning might very well be below threshold because of a large pump detuning. In fact, the analysis of Section 3 should then be reworked and reformulated in terms of coincidences of three resonances instead of two. It is not certain that this more complicated problem admits solutions.

To conclude, an OPO designed in order to observe the Hopf bifurcation should have a short cavity (e.g., monolithic setup), high birefringence and pumping rate. The pump cavity finesse should be as high as possible. Under these conditions, however, an OPO would be very difficult to operate and to stabilize on an operating point. Even then, the numerical analysis of Section 4 indicates that unstable zones would remain small compared to the range of operating parameters. This casts serious doubts on the experimental observability of the Hopf bifurcation of the monomode mean-field model.

6 Conclusion

In this paper we have raised the issue that contrary to what is commonly assumed in theoretical studies of the dynamics of optical parametric oscillators, signal detuning is not a parameter that can be arbitrarily fixed, as its value results from a complex selection process. Thus, detuning limitation due to mode hopping may affect the occurrence of dynamical instabilities occurring at high values of the detuning. As a simple example, we analyzed under which conditions the Hopf bifurcation leading to periodic behavior in the monomode mean-field model of a triply resonant OPO can be observed.

We first showed that signal detuning must reach a minimal value for the bifurcation to occur, even at infinite pump power. We then described how the mechanism of mode hopping restraints the values signal detuning can take and we gave an analytical expression of the maximal detuning allowed by mode hopping. By comparing the two bounds so obtained, we showed that they are incompatible in many configurations, showing that finite pump power is not necessarily the limiting factor for observing this instability. This was confirmed in numerical computations of instability domains carried out at a finite pump power corresponding to our experimental configuration, in which we observed that most of the unstable domains are inaccessible because of mode hopping. We found that pump finesse is a critical parameter that should be made as large as possible in order to observe the Hopf bifurcation. However experimental setups designed for this purpose should most certainly be extremely difficult to operate.

For the sake of simplicity, our derivation of the maximal detuning allowed by mode hopping relied on two main hypotheses. One was that signal and idler have frequencies close to 1:1 ratio but experience different indices, as in our type-II experiments. Generalization to other frequency ratios in the type-II configuration should be straightforward and is not expected to modify the conclusions of the present work. Type-I OPOs near frequency degeneracy have more complex tuning properties and should be analyzed separately. The other hypothesis was that parametric gain can be considered constant along a frequency domain containing many longitudinal modes so that the lowest possible detuning is always selected. If that is not the case, then values of signal detuning higher than predicted may be obtained and our analysis would have to be adapted. However, it does not seem likely that our conclusions would be modified a lot.

An open question is whether conclusions drawn for the Hopf bifurcation of the monomode mean-field model also hold for other theoretical predictions of temporal or pattern-forming instabilities in doubly or triply optical parametric oscillators. Such instabilities have often been reported for high values of the pumping rate, comparable pump and signal finesse, and for values of signal detuning generally above the cavity resonance half width (see, e.g., references [6–9]). Since pump finesse is usually much smaller that signal finesse in realistic experimental setups, it would be interesting to determine whether decreasing pump finesse increases the minimum detuning value at which these instabilities appear, as is the case for the Hopf instability we have studied in this paper and as it seems to be for other instabilities (see e.g., Fig. 1 in [10]). If this is so, their observability would then also be affected by detuning limitations due to mode hopping rather than by finiteness of pump power. A detailed comparison of instability thresholds in detuning space with the maximum values allowed by mode hopping is therefore needed to assess the experimental relevance of these theoretical predictions.

Thus, mode hopping is not only a nuisance for stabilizing and tuning OPOs but also for using them as tools to study complex dynamical behavior. However, the conclusion of our study may not be as pessimistic as it seems, as it provides guidelines for designing experimental setups where the Hopf instability could be finally observed, such as with a very short cavity.

We are most grateful to S. Bielawski, D. Derozier, P. Suret, and J. Zemmouri for stimulating discussions. The Centre d'Études et de Recherches Lasers et Applications is supported by the Ministère chargé de la Recherche, the Région Nord-Pas de Calais and the Fonds Européen de Développement Économique des Régions.

References

1. Special issue on $\chi^{(2)}$ second order nonlinear optics, Quant. Semiclass. Opt. **9** (1997)
2. K. McNeil, P. Drummond, D. Walls, Opt. Commun. **27**, 292 (1978)
3. P. Drummond, K. McNeil, D. Walls, Opt. Acta **27**, 321 (1980)
4. L.A. Lugiato, C. Oldano, C. Fabre, E. Giacobino, R.J. Horowicz, Nuovo Cim. D **10**, 959 (1988)
5. G. Oppo, M. Brambilla, L. Lugiato, Phys. Rev. A **49**, 2028 (1994)
6. K. Staliunas, J. Mod. Opt. **42**, 1261 (1995)

7. M. Marte, H. Ritsch, K. Petsas, A. Gatti, L. Lugiato, C. Fabre, D. Leduc, Opt. Expr. **3**, 71 (1998)
8. C. Schwob, P. Cohadon, C. Fabre, M. Marte, H. Ritsch, A. Gatti, L. Lugiato, Appl. Phys. B **66**, 685 (1998)
9. M. Tlidi, M.L. Berre, E. Ressayre, A. Tallet, L.D. Menza, Phys. Rev. A **61**, 043806 (2000)
10. G. Oppo, A. Scroggie, D. Sinclair, M. Brambilla, J. Mod. Opt. **47**, 2005 (2000)
11. C. Richy, K.I. Petsas, E. Giacobino, C. Fabre, L. Lugiato, J. Opt. Soc. Am. B **12**, 456 (1995)
12. P. Suret, D. Derozier, M. Lefranc, J. Zemmouri, S. Bielawski, Phys. Rev. A **61**, 021805(R) (2000)
13. P. Suret, M. Lefranc, D. Derozier, J. Zemmouri, S. Bielawski, Opt. Lett. **26**, 1415 (2001)
14. P. Suret, M. Lefranc, D. Derozier, J. Zemmouri, S. Bielawski, Opt. Commun. **200**, 369 (2001)
15. A. Amon, M. Lefranc, Phys. Rev. Lett. **92**, 094101 (2004)
16. R. Eckardt, C. Nabors, W. Koslovsky, R. Byer, J. Opt. Soc. Am. B **8**, 646 (1991)
17. T. Debuisschert, A. Sizmann, E. Giacobino, C. Fabre, J. Opt. Soc. Am. B **10**, 1668 (1993)
18. M.J. Padgett, F.G. Colville, M.H. Dunn, IEEE J. Quant. Electron. **30**, 2979 (1994)
19. A. Henderson, M. Padgett, F. Colville, J. Zhang, M. Dunn, Opt. Commun. **119**, 256 (1995)
20. C. Fabre, P.F. Cohadon, C. Schwob, Quant. Semiclass. Opt. **9**, 165 (1997)
21. A. Amon, M. Nizette, M. Lefranc, T. Erneux, Phys. Rev. A **68**, 023801 (2003)
22. R.W. Boyd, *Nonlinear Optics*, 2nd edn. (Academic Press, 2003)
23. A. Yariv, W. Louisell, IEEE J. Quant. Electron. **QE-2**, 418 (1966)